January 2006

Predictions and Performances of Prefabricated Vertical Drain Stabilised Soft Clay Foundations

Buddhima Indraratna
University of Wollongong, indra@uow.edu.au

Cholachat Rujikiatkamjorn
University of Wollongong, cholacha@uow.edu.au

Predictions and performances of prefabricated vertical drain stabilised soft clay foundations

Buddhima Indraratna
Professor, Division of Civil Engineering, University of Wollongong, City of Wollongong, NSW 2522, Australia.

Cholachat Rujikiatkamjorn
Associate Research Fellow, Division of Civil Engineering, University of Wollongong, City of Wollongong, NSW 2522, Australia.

ABSTRACT: In this paper, the analytical solution for radial consolidation of soft soils is proposed considering the impacts of the variation of volume compressibility and permeability. The Cavity Expansion Theory is employed to predict the smear zone caused by the installation of mandrel driven vertical drains in soft clay. The smear zone prediction is then compared to the data obtained from the large-scale radial consolidation tests. Furthermore, the advantages and limitations of vacuum application through vertical drains in the absence of high surcharge embankments are discussed using the proposed solutions. The applied vacuum pressure generates negative pore water pressure, resulting in an increase in the effective stress, which leads to accelerated consolidation. Analytical and Numerical analysis incorporating the equivalent plane strain solution are conducted to predict the excess pore pressures, lateral and vertical displacements. The equivalent plane strain solution can be used as a predictive tool with acceptable accuracy due to the significant progress that has been made in the past few years through rigorous mathematical modelling and numerical analysis developed by the primary author and co-workers (Indraratna et al., 1992 – 2005).

Several case histories are discussed and analysed, including the site of the 2nd Bangkok International Airport. The predictions are compared with the available field data, confirming that the equivalent plane strain model can be used confidently to predict the performance with acceptable accuracy. Difficulties in assuring good performance can also be analysed and interpreted through mathematical modelling, thereby enabling due caution in the design and construction stages. The research findings verify that the role of smear, drain unsaturation, and vacuum distribution can significantly affect soil consolidation, hence, these aspects need to be modelled appropriately in any numerical analysis to obtain reliable predictions.

1 INTRODUCTION

Rapid urban development has compelled engineers to construct earth structures such as major highways and railways over soft clay deposits which usually show excessive settlement and low bearing capacity characteristics (Johnson, 1970; Indraratna et al., 1992). In the coastal regions of many countries, soft clays are widespread in the vicinity of capital cities. When such areas are selected for infrastructure development, ground improvement techniques for the underlying soft soils is essential. The application of prefabricated vertical drains (PVDs) with preloading has become common practice, and it is one of the most effective soft clay improvement methods. Usually, a surcharge load equal to or greater than the expected foundation loading is applied over the soil surface to accelerate consolidation by rapid pore pressure dissipation through the vertical drains (Hansbo, 1981; Jamiolkowski, 1983; Indraratna et la., 1994; Indraratna and Redana., 2000).

Figure 1 illustrates a typical plan of vertical drain system installation and essential instruments required to monitor the performance of soil foundation beneath an earthfill embankment. Before installing the vertical drains, general site preparations including the removal of vegetation and surficial soil, establishing site grading and placing a compact sand blanket are nominally required. The sand blanket is employed to expel water away from the drains and to provide a sound-working mat for the vertical drain rigs.

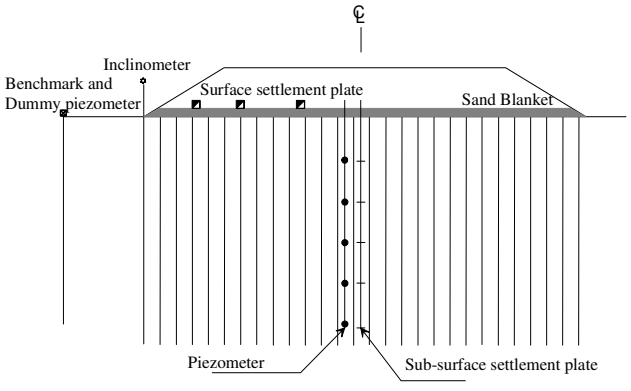

Figure 1: Vertical drain system with preloading (Indraratna et al. 2005d).

In order to increase vertical drain system performance, the vacuum preloading method was initially introduced in Sweden by Kjellman (1952) for cardboard wick drains. It has been used extensively to accelerate the consolidation process for improving soft ground, such as Tianjin port, China (Yan and Chu, 2003). When a higher surcharge load is required to meet the expected settlement and the cost of surcharge becomes costly, a combined vacuum and fill surcharge can be employed (Cognon et al., 1994; Indraratna et al. 2005a). In areas of very soft clay, where a high surcharge embankment cannot be raised, the vacuum application remains the ideal choice. Recently, the PVD system has also been employed to distribute vacuum pressure to deep subsoil layer, thereby increasing the

consolidation rate of reclaimed land from the sea (e.g. Qian et al., 1992; Chu et al., 2000; Tang and Shang, 2000).

To investigate the behaviour of vertical drains, the unit cell theory representing a single circular drain surrounded by a soil annulus in an axisymmetric condition has usually been used (e.g. Barron, 1948; Yoshikuni and Nakanodo, 1974; Hansbo, 1981). Under embankment loading, vertical drains not only accelerate the consolidation rate, but also influence the deformation pattern of the subsoil. It is only at the embankment centreline where lateral displacements are zero that the unit cell analysis provides acceptable accuracy. Elsewhere, especially towards the embankment toe, single drain analysis cannot provide an accurate prediction due to lateral yield and heave compared to plane strain multi-drain analysis (Indraratna, et al., 1997).

Modelling of prefabricated vertical drains in plane strain finite element analysis has become popular (Hird et al., 1992, Indraratna et al., 2004). The basic principle is to match the average degree of radial consolidation in axisymmetric condition with the proposed equivalent plane strain analysis. This equivalence enhances computational efficiency by reducing the convergence time and required computer memory, while still providing the correct time-settlement response. Various researchers have described the advantage of such plane strain solutions for field studies where a large number of drains are used, for which a true 3D analysis may become cumbersome or impractical (e.g. Hird et al., 1992, Chai et al., 1995, Indraratna et al., 2005f).

In this paper, the smear zone prediction based on The Cavity Expansion Theory is discussed based on the large scale laboratory results. The effects of the compressibility indices, the variation of soil permeability and the magnitude of preloading are examined through the consolidation process. The equivalent 2-D plane strain solution is described which includes the effects of smear zone caused by mandrel driven vertical drains. The equivalent (transformed) permeability coefficients are incorporated in finite element codes, employing the modified Cam-clay theory. Numerical analysis is conducted to predict the excess pore pressures, lateral and vertical displacements. Two case histories are discussed and analysed, including the site of the New Bangkok International Airport (Thailand) and the predictions are compared with the available field data. The research findings verify that the impact of smear and vacuum pressure can significantly affect soil consolidation, hence, in order to obtain reliable consolidation predictions, these aspects need to be simulated appropriately in the selected numerical approach.

2 DEVELOPMENT OF THE THEORY OF CONSOLIDATION WITH VERTICAL DRAINAGE AND VACUUM PRELOADING

During the consolidation process, both volume compressibility and permeability vary according to the stress level, which imparts a direct influence on the shape of e-logσ' and e-logk_h relationships (Lekha et al. 2003). Moreover, the nature of subsoil stress history (preconsolidation pressure) gives different consolidation responses (Seah and Juirnarongrit 2003). Therefore, in order to obtain the accurate prediction of the behaviour of a vertical drain system, Indraratna et al. (2005b) have incorporated the relationships of e-logσ' and e-logk_h with radial consolidation.

2.1 *Key assumptions*

The following assumptions are based on the equal vertical strain solution given by Hansbo (1981) and the variation of soil permeability and soil volume compressibility. The following is a summary taken from Indraratna et al. (2005b).

(1) Soil is homogeneous and fully saturated, whereby Darcy's law is adopted. At the outer boundary of the unit cell, flow is not permitted to occur. For relatively long vertical drains, only radial flow is allowed (i.e. no vertical flow).

(2) Soil strain is uniform at the upper boundary of the unit cell and the small strain theory is valid.

(3) The relationship between the average void ratio and the logarithm of average effective stress in the normally consolidated range (Fig. 2) can be expressed by: $\bar{e} = e_0 - C_c \log(\sigma'/\sigma'_i)$. If the current vertical effective stress (σ') is less than p'_c, then for the overconsolidated range, the recompression index (C_r) is used rather than C_c.

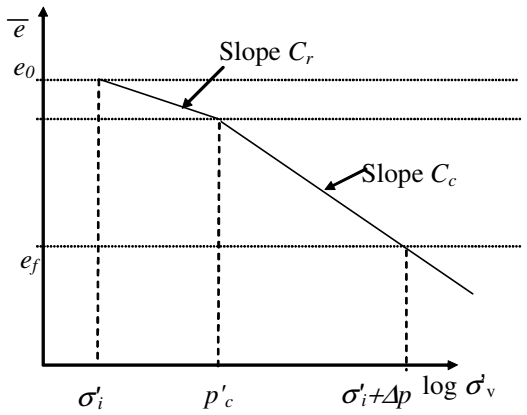

Figure 2: Soil compression curve (after Indraratna et al., 2005b)

(4) For radial drainage, the horizontal permeability of soil decreases with the average void ratio (Fig. 3). The relationship between these two parameters is given by Tavenas et al. (1983): $\bar{e} = e_0 + C_k \log(k_h / k_{hi})$ The permeability index (C_k) is generally considered to be inde-

pendent of stress history (p'_c) as explained by Nagaraj et al. (1994).

(5) The vacuum pressure distribution along the drain boundary is considered to vary linearly from - p_0 at top of the drain to - $k_1 p_0$ at the bottom of the drain, where k_1 is a ratio between vacuum pressure at the bottom and the top of the drain (Fig. 4).

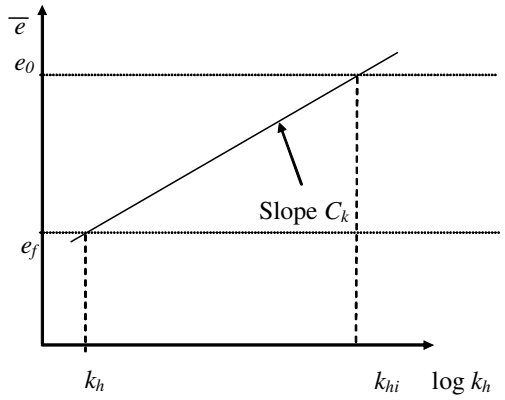

Figure 3: Semi-log permeability-void ratio (after Indraratna et al., 2005b)

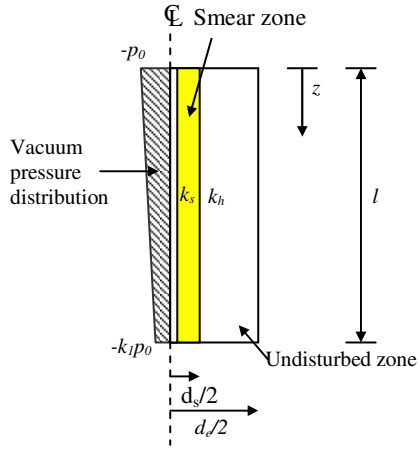

Figure 4: An axisymmetric unit cell with vacuum pressure distribution (modified after Indraratna et al., 2005c)

2.2 *Solution for an axisymmetric unit cell*

According to Indraratna et al. (2005b), the dissipation rate of average excess pore pressure ratio ($R_u = \bar{u}_t / \Delta p$) at any time factor ($T_h$) can be expressed as:

$$\frac{\partial\left(R_u + \frac{p_0}{\Delta p}\frac{(1+k_1)}{2}\right)}{\partial T_h} = -\frac{8}{\mu}\frac{m_{vi}}{m_v}\frac{k_h}{k_{hi}}\left(R_u + \frac{p_0}{\Delta p}\frac{(1+k_1)}{2}\right) \quad (1)$$

The void ratio (e)-effective stress (σ') and the void ratio-permeability relations for normally consolidated clays can be express as (Tavenas et al., 1983):

$$\bar{e} = e_0 - C_c \log(\sigma'/\sigma'_i) \quad (2)$$

$$\bar{e} = e_0 + C_k \log(k_h/k_{hi}) \quad (3)$$

where, C_c is the compression index and C_k is the permeability index ($C_k \approx 0.5 e_o$). If the current vertical effective stress (σ') is smaller than preconsolidation pressure (p'_c), the recompression index (C_r) is used instead of C_c for the overconsolidated range.

Differentiating Eq. (2) with respect to the effective stress (σ') gives:

$$m_{vi}/m_v = 1 + \Delta p/\sigma'_i - R_u \Delta p/\sigma'_i \quad (4)$$

Combining Eqs. (3) and (4) yields:

$$k_h/k_{hi} = \left(1 + \Delta p/\sigma'_i - R_u \Delta p/\sigma'_i\right)^{-C_c/C_k} \quad (5)$$

Substituting Eqs. (4) and (5) into (1) gives:

$$\partial\left(R_u + \frac{p_0}{\Delta p}\frac{(1+k_1)}{2}\right)\Big/\partial T_h = -8P\left(R_u + p_0(1+k_1)/2\Delta p\right)/\mu \quad (6)$$

where, $P = \left(1 + \Delta p/\sigma'_i - R_u \Delta p/\sigma'_i\right)^{1-C_c/C_k}$

It can be seen that Eq. (6) is a non-linear partial differential equation for radial consolidation under immediate loading, incorporating the e-logσ' and e-logk_h relations. The nonlinear differential Eq. (6) with variable R_u does not have a general solution and, P varies between 1 and the value of $\left(1 + \Delta p/\sigma'_i + p_0(1+k_1)/2\sigma'_i\right)^{1-C_c/C_k}$. Hence, an average value for P is adopted:

$$P = P_{av} = 0.5\left[1 + \left(1 + \Delta p/\sigma'_i + p_0(1+k_1)/2\sigma'_i\right)^{1-C_c/C_k}\right] \quad (7)$$

Integrating Eq. (6) after incorporating Eq. (7) subjected to the boundary condition that R_u = 1.0 at T_h=0, gives the following algebraic expression:

$$R_u = \left(1 + \frac{p_0}{\Delta p}\frac{(1+k_1)}{2}\right)\exp\left(\frac{-8T_h^*}{\mu}\right) - \frac{p_0}{\Delta p}\frac{(1+k_1)}{2} \quad (8)$$

where, $T_h^* = P_{av} T_h$ (9)

When the value of C_c/C_k approaches unity and p_0 becomes zero, the authors' solution converges to the conventional solution proposed by Hansbo (1981):

$$R_u = \exp(-8T_h/\mu) \quad (10a)$$

in which,

$$\mu = ln\frac{n}{s} + \frac{k_h}{k_s} ln\, s - 0.75 \qquad (10b)$$

where, μ = a group of parameters representing the geometry of the vertical drain system and smear effect, $n = d_e/d_w$, $s = d_s/d_w$, d_e = equivalent diameter of cylinder of soil around drain, d_s = diameter of smear zone and d_w = diameter of drain well. In Eq. (10b), k_h = average horizontal permeability in the undistrubed zone (m/s), and k_s = average horizontal permeability in the smear zone (m/s). T_h is the dimensionless time factor for consolidation due to radial drainage.

Substituting T_h * in Eq. (8), the expression for excess pore pressure ratio for normally consolidated clay becomes:

$$R_u = \exp\left(-4\left[1 + \left\{ 1 + \frac{\Delta p}{\sigma'_i} \right\}^{1-C_c/C_k} \right] \frac{T_h}{\mu} \right) \qquad (11a)$$

For overconsolidated soil, $\sigma' < p'_c$ (e.g. topmost layer close to surface)

$$R_u = \exp\left(-4\left[1 + \left\{ 1 + \frac{\Delta p}{\sigma'_i} \right\}^{1-C_r/C_k} \right] \frac{T_h}{\mu} \right) \qquad (11b)$$

When the effective stress equals the preconsolidation pressure ($\sigma' < p'_c$), the corresponding time factor $T_{h,pc}$ can then be determined by:

$$T_{h,pc} = \frac{\mu}{4\left[1 + \left\{ 1 + \frac{\Delta p}{\sigma'_i} \right\}^{1-C_r/C_k} \right]} \ln\left(\frac{\Delta p}{\sigma'_i + \Delta p - p'_c} \right) \qquad (11c)$$

When $\sigma' > p'_c$ along the slope of the normally consolidation curve (C_c), the expression for excess pore pressure ratio when $T_h > T_{h,pc}$ is given by:

$$R_u = \left(\frac{\sigma'_i + \Delta p - p'_c}{\Delta p} \right) \exp\left(-4\left[1 + \left\{ 1 + \frac{\sigma'_i + \Delta p - p'_c}{p'_c} \right\}^{1-C_c/C_k} \right] \frac{\left(T_h - T_{h,pc}\right)}{\mu} \right) \qquad (11d)$$

where, $T_h = \frac{c_{h,pc} t}{d_e^2}$, $c_{h,pc} = c_{hi}\left(\frac{p'_c}{\sigma_i'} \right)^{1-C_r/C_k}$

Since the relationship between effective stress and strain is non-linear, the average degree of consolidation can be described either based on excess pore pressure (stress) (U_p) or based on strain (U_s). U_p indicates the rate of dissipation of excess pore pressure whereas U_p shows the rate of development of the surface settlement. Normally, $U_p \neq U_s$ except when the effective stress and strain is a linear relationship, which is in accordance with Terzaghi's one-dimensional theory. Therefore, the average degree of consolidation based on excess pore pressure can be obtained as follows:

$$U_p = 1 - R_u \qquad (12)$$

The average degree of consolidation based on settlement (strain) is defined by:

$$U_s = \frac{\rho}{\rho_\infty} \qquad (13)$$

The associated settlements (ρ) are then evaluated by the following equations:

$$\rho = \frac{HC_r}{1+e_0} \log\left(\frac{\sigma'}{\sigma'_i} \right), \qquad \sigma'_i \le \sigma' \le p'_c \qquad (14a)$$

$$\rho = \frac{H}{1+e_0}\left[C_r \log\left(\frac{p'_c}{\sigma'_i} \right) + C_c \log\left(\frac{\sigma'}{p'_c} \right) \right], \qquad p'_c \le \sigma' \le \sigma'_i + \Delta p \qquad (14b)$$

$$\rho = \frac{HC_c}{1+e_0} \log\left(\frac{\sigma'}{\sigma'_i} \right) \text{ for normally consolidated clay} \qquad (14c)$$

It is noted that ρ_∞ can be obtained by substituting $\sigma' = \sigma'_i + \Delta p$ into the above equations.

In the above equations, ρ = settlement at a given time, ρ_c = total primary consolidation settlement, C_c = compression index, C_r = recompression index and H = compressible soil thiskness.

Depending on the location of the initial and final effective stresses with respect to the normally consolidated and overconsolidated domains, the following is a summary of the relavant computational steps.

If both the initial and final effective stresses are in the normally consolidated range, Eqs (11a) and (12) are employed to calculate U_p, whereas Eqs. (13) and (14c) are used to compute U_s.

If both the initial and final effective stresses are in the overconsolidated range, Eqs. (11b) and (12) are employed

to calculate U_p, and Eqs. (13) and (14a) are used to determine U_s.

If the initial effective stress falls on the overconsolidated domain and the final effective stress is on the normally consolidated domain, then Eqs. (11b)-(11d) and (12) are employed to calculate U_p, Eqs. (13) (14a) and (14b) are employed to calculate U_s.

3 EQUIVALENT PLANE STRAIN CONSOLIDATION MODEL

Most finite element analyses on embankments are carried out based on the 2D plane strain assumption. However, the consolidation around vertical drains is mainly axisymmetric. Therefore, to employ a realistic 2-D finite element analysis for vertical drains, the *equivalence* between the plane strain analysis and axisymmetric analysis needs to be established. Indraratna and Redana (1997, 1998, 2000) and Indraratna et al. (2005a) converted the vertical drain system shown in Fig. 5 into an equivalent parallel drain well by adjusting the coefficient of permeability of the soil, and by assuming the plane strain cell (a width of 2*B)*. The half width of the drain b_w and half width of the smear zone b_s may be kept the same as their axisymmetric radii r_w and r_s, respectively, which suggests $b_w = r_w$ and $b_s = r_s$.

Indraratna et al. (2005a) represented the average degree of consolidation in plane strain condition as follows:

$$\frac{\bar{u}}{\bar{u}_0} = \left(1 + \frac{p_{0p}}{\bar{u}_o}\frac{(1+k_1)}{2}\right)\exp\left(-\frac{8T_{hp}}{\mu_p}\right) - \frac{p_{0p}}{\bar{u}_0}\frac{(1+k_1)}{2} \quad (15)$$

and

$$\mu_p = \left[\alpha + (\beta)\frac{k_{hp}}{k'_{hp}}\right] \quad (16)$$

where, $\bar{u}_0$ = initial excess pore pressure, $\bar{u}$ = pore pressure at time t (average values) and T_{hp} = time factor in plane strain., k_{hp} and k'_{hp} are the undisturbed horizontal and the corresponding smear zone equivalent permeabilities, respectively. The geometric parameters α and β, are given by:

$$\alpha = \frac{2}{3} - \frac{2b_s}{B}\left(1 - \frac{b_s}{B} + \frac{b_s^2}{3B^2}\right) \quad (17a)$$

$$\beta = \frac{1}{B^2}(b_s - b_w)^2 + \frac{b_s}{3B^3}\left(3b_w^2 - b_s^2\right) \quad (17b)$$

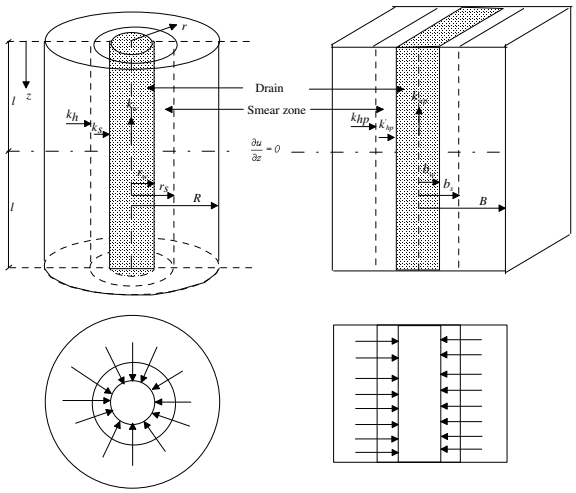

(a) Axisymmetric (b) Plane strain

Figure 5: Conversion of an axisymmetric unit cell into plane strain condition (after Indraratna and Redana, 2000)

At a given effective stress level and at each time step, the average degree of consolidation for both axisymmetric ($\bar{U}_p$) and equivalent plane strain ($\bar{U}p, pl$) conditions are made equal, hence:

$$\bar{U}_p = \bar{U}_{p,pl} \quad (18)$$

Combining Eqs. 15 and 17 with Eq. 10 of original Hansbo theory (Hansbo, 1981), the time factor ratio can be represented by the following equation:

$$\frac{T_{hp}}{T_h} = \frac{k_{hp}}{k_h}\frac{R^2}{B^2} = \frac{\mu_P}{\mu} \quad (19)$$

By assuming the magnitudes of *R* and *B* to be the same, Indraratna and Redana (2000) presented a relationship between k_{hp} and k'_{hp}, as follows:

The influence of smear effect can be modelled by the ratio of the smear zone permeability to the undisturbed permeability, as follows:

$$\frac{k'_{hp}}{k_{hp}} = \frac{\beta}{\frac{k_{hp}}{k_h}\left[\ln\left(\frac{n}{s}\right) + \left(\frac{k_h}{k'_h}\right)\ln(s) - 0.75\right] - \alpha} \quad (20)$$

If smear and well resistance effects are ignored in the above expression, then the simplified ratio of plane strain to axisymmetric permeability is readily obtained, as also proposed earlier by Hird et al. (1992):

$$\frac{k_{hp}}{k_h} = \frac{0.67}{[\ln(n) - 0.75]} \quad (21)$$

For vacuum preloading, the equivalent vacuum pressure in plane strain and axisymmetric are the same.

4 EVALUATION OF SMEAR ZONE SURROUNDING MANDREL DRIVEN VERTICAL DRAINS USING CAVITY EXPANSION ANALYSIS

Indraratna et al. (2005g) and Sathananthan (2005) have made an attempt to estimate the extent of "smear zone", caused by mandrel installation using the Cylindrical Cavity Expansion theory incorporating the modified Cam-clay model (MCC). This technique is commonly used to analyse pile driving, tunnelling and soil testing. When a mandrel is driven into soil, it will initially displace a volume of soil equal to the volume of the mandrel. A heave of soil can occur at the soil surface, up to about ten times the radius of the mandrel. At a greater depth, the soil is displaced predominantly outwards in the radial direction. Therefore, the expansion of a cylindrical cavity with a final radius equal to that of the mandrel is appropriate to predict the extent of smear zone.

The following is the summary from the doctoral research of Sathananthan (2005). After the initial yielding at the cavity wall, a zone of soil extending from the cavity wall to a radial distance (r_p) will become plastic as the cavity pressure continues to increase (Figure 6). For a soil obeying the MCC model, the yielding criterion is given by:

$$\eta = \mathrm{M}\sqrt{\frac{p_c'}{p'} - 1} \tag{22}$$

where, η = stress ratio q/p' (q is the deviatoric stress $(\sigma_1-\sigma_3)/2$ and p' is the effective mean stress $(\sigma_1+2\sigma_3)/3$), M = slope of critical state line projected to q-p' plane and p'_c = effective preconsolidation pressure.

The stress ratio at the elastic-plastic boundary can be found as follows:

$$\eta_p = \left(\frac{q}{p'}\right)_{r=r_p} = \frac{q_p}{p_0'} = \mathrm{M}\sqrt{OCR-1} \tag{23}$$

where, η_p = stress ratio at the elastic-plastic boundary, r = distance from central axis of the drain, $q_p = (\sigma_1-\sigma_3)/2$ at the elastic-plastic boundary and OCR is the isotropic over consolidation ratio, defined by p_{c0}'/p_0' (p_{c0}' is the initial preconsolidation pressure and p_0' is the initial effective mean stress). Stress ratio at any point can be determined as follows:

$$\ln\left(1-\frac{\left(a^2-a_0^2\right)}{r^2}\right) = -\frac{2(1+\nu)}{3\sqrt{3}(1-2\nu)}\frac{\kappa}{\upsilon}\eta - 2\sqrt{3}\,\frac{\kappa\Lambda}{\upsilon \mathrm{M}}\,f(\mathrm{M},\eta,OCR) \tag{24}$$

and

$$f(\mathrm{M},\eta,OCR) = \frac{1}{2}\ln\left[\frac{(\mathrm{M}+\eta)\left(1-\sqrt{OCR-1}\right)}{(\mathrm{M}-\eta)\left(1+\sqrt{OCR-1}\right)}\right] - \tan^{-1}\left(\frac{\eta}{\mathrm{M}}\right) + \tan^{-1}\left(\sqrt{OCR-1}\right) \tag{25}$$

where, a = radius of the cavity, a_0 = initial radius of the cavity, ν = Poisson's ratio, κ = slope of the overconsolidation line, υ = specific volume and $\Lambda = 1-\kappa/\lambda$ (λ is the slope of the normal consolidation line). Finally, the corresponding mean effective stress, in terms of deviatoric stress, total stress and excess pore pressure, can be expressed by the following expressions:

$$p' = p_0'\left[\frac{OCR}{1+(\eta/\mathrm{M})^2}\right]^{\Lambda} \tag{26}$$

$$q = \eta\, p' \tag{27}$$

$$p = \sigma_{rp} - \frac{q}{\sqrt{3}} + \frac{2}{\sqrt{3}}\int_r^{r_p}\frac{q}{r}dr \tag{28}$$

Employing Equations (26)-(28), the excess pore pressure due to mandrel driving (Δu) can be determined by:

$$\Delta u = (p-p_0) - (p'-p_0') \tag{29}$$

where, p_0 = initial total mean stress. The extent of the smear zone can be suggested as the region in which the excess pore pressure is higher than the initial overburden pressure (σ_{v0}') (Fig. 6). This is because, in this region, the soil properties, such as permeability and soil anisotropy, are disturbed severely at radial distance where $\Delta u = \sigma_{v0}'$.

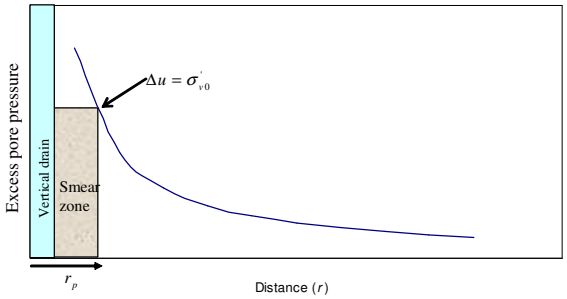

Figure 6: Smear zone prediction by the Cavity Expansion Theory

5 LABORATORY TESTING USING LARGE-SCALE CONSOLIDOMETER

At the University of Wollongong, the performance of prefabricated vertical drains has been extensively studied by employing large-scale laboratory consolidation tests (Fig. 7). Initially, this apparatus was developed by Indraratna and Redana (1995,1997) to study the effect of smear due to vertical drain installation including sand drains and prefabricated vertical drains (PVDs). The apparatus was later modified to accommodate the vacuum application (Indraratna et al. 2004). The internal radius and the overall height of the assembled cell are 225 mm and 1000 mm, respectively. The loading system was applied by an air jack compressor system via a piston. The settlement was measured by a Linear Variable Differential Transducer (LVDT) placed at the top of this piston. An array of strain gauge type pore pressure transducers complete with wiring to supply recommended 10 V DC supply was installed to measure the excess pore water pressures at various points.

5.1 *Smear zone determination due to vertical drain installation*

Indraratna and Redana (1997) found that even though a larger width of the drain may cause a greater smear zone, for PVDs, the measurements and predictions indicate slightly increasing settlements due to the increased surface area, facilitating efficient pore water pressure dissipation. The smear zone extent can be determined either by permeability variation or water content variation along the radial distance (Indraratna and Redana, 1997; Sathananthan and Indraratna, 2006). Figure 8 shows the variation of the ratio of the horizontal to vertical permeabilities (k_h/k_v) at different consolidation pressures along the radial distance, obtained from large-scale laboratory consolidation. The variation of the water content with depth and radial distance is shown in Figure 9 for an applied pressure of 200 kPa. As expected, the water content decreases towards the drain, and also the water content is greater towards the bottom of cell at all radial locations.

Based on these curves, the extent of smear zone can be estimated to be around 2.5 times the equivalent mandrel radius. This agrees well with the estimated extent of smear zone based on both the k_h/k_v ratio (Fig. 8). It can be seen that the average value of k_h/k_v starts to decrease considerably from 1.65 (outside smear zone) to 1.1 (inside smear zone). It implies that the permeability ratio between undisturbed and smear zone (k_h/k'_h) is approximately 1.5 and the extent of smear zone (r_s) is 4-5 times the radius of the vertical drain (r_w). It should be noted that k_h/k'_h ratio in the field can vary from 1.5 to 10, depending on the type of drain and soils as well as installation procedures (Saye, 2003).

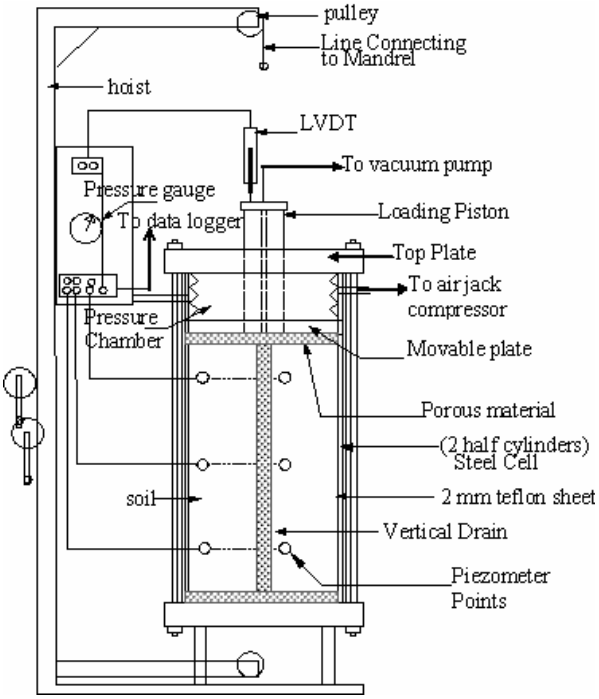

Figure 7: Schematic of large-scale consolidation apparatus (after Indraratna and Redana, 1995)

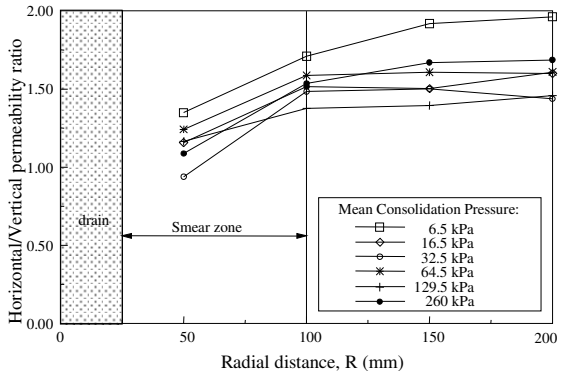

Figure 8: Ratio of k_h/k_v along the radial distance from the central drain (after Indraratna and Redana, 1995)

5.2 *Effects of vacuum preloading*

Indraratna et al. (2004) studied the effects of application of vacuum pressure through prefabricated vertical band drains (PVDs). The vacuum pressure was set to 100 kPa and applied to the PVD and soil surface through the central hole of the rigid piston. The subsequent surcharge load was applied instantaneously in two stages, 40 kPa and 100 kPa with duration of 14 days between each stage. During the test, the vacuum pressure was released in two stages for short periods to investigate the effects of vacuum unloading and reloading. The suction measured close

to the PVD and the surface settlement measured from LVDT are shown in Figure 10.

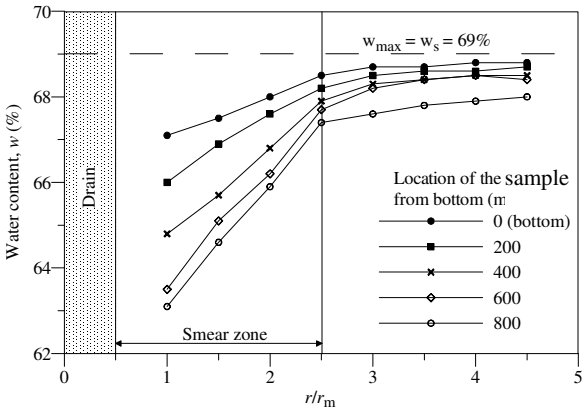

Figure 9: Variation of water content with depth and radial distance for an applied pressure of 200 kPa (after Sathananthan and Indraratna, 2006)

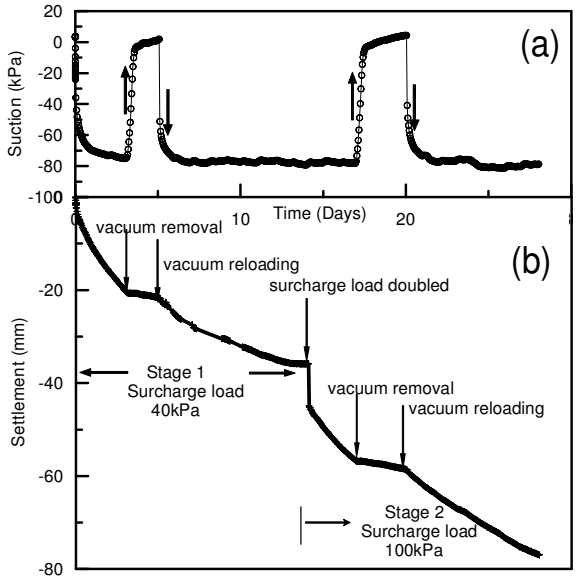

Figure 10: a) Suction in the drain (240mm from bottom) and b) surface settlement surface settlement associated with simulated vacuum loading and removal (Indraratna et al. 2004)

This also indicates that the suction head decreases with the drain depth, as the maximum suction of 100 kPa could not be maintained along the entire drain length. The settlement associated with combined vacuum and surcharge load is shown in Figure 10b, and it clearly reflects the effect of vacuum removal and re-application by the corresponding change of gradient of the settlement plot (Indraratna et al. 2004).

6 PERFORMANCE OF TEST EMBANKMENT STABILISED WITH VERTICAL DRAINS INCORPORATING VACUUM PRESSURE ON SOFT CLAY, BANGKOK, THAILAND

6.1 *General*

The Second Bangkok International Airport or Suvarnabhumi Airport is situated about 30km from the city of Bangkok. In the past, the site was occupied by rice fields for for agricultural purposes. The area is often flooded during the rainy season and the soil generally has very high moisture content. Therefore, soft marine clays, often present considerable construction problems, which require ground improvement techniques to prevent excessive settlement and lateral movement.

The subsoil profile at the site consists of 1m thick weathered crust (highly overconsolidated clay) overlying a very soft to medium clay, which extends about 10m below the ground surface. Underneath the medium clay layer, a light-brown stiff clay layer is found at a depth of 10-21m (AIT, 1995). The ground-water level fluctuates between 0.5 and 1.5m below the surface. The water content of the very soft clay layer varies from 80 to 100%, whereas in the lower parts of the stratification (10-14m) it changes from 50 to 80%. The plastic limits and liquid limits of the soil in each layer are similar and found to be in the range of 80 to 100% and 20 to 40%, respectively.

6.2 *Embankment details and vacuum pressure measurement*

Several trial embankments were built at this site, two of which, (TV1 and TV2) were built with PVDs and vacuum application (Asian Institute of Technology, 1995). Total base area of each embankment was 40×40 m^2. Figures 11 and 12 present the vertical cross sections and field instruments positions for embankments TV1 and TV2, respectively. For TV1 (Fig. 11), 15m long PVDs with a hypernet drainage system were installed, and for TV2 (Fig. 12), 12m long PVDs with perforated and corrugated pipes wrapped together in non-woven geotextile were used. The drainage blanket (working platform) was constructed with sand 0.3 m and 0.8 m for embankments TV1 and TV2, respectively with an air and water tight Linear Low Density Polyethylene (LLDPE) geomembrane liner placed on top of the drainage system. This liner was sealed by placing its edges at the bottom of the trench perimeter and covered with a 300mm layer of bentonite and then submerged with water. The array of instrumentation of the embankments includes piezometers, surface settlement plates, multipoint extensometers, inclinometers, observation wells and benchmarks.

Table 1 shows the vertical drain properties for embankment TV1 and TV2. The PVDs were installed in a triangular pattern at a spacing of 1m. The type of drain in-

stalled in both embankments is Mebra drains (100 mm x 3 mm). In these embankments, the drains were installed using a mandrel, which was gradually pushed into the soil by a static weight without any vibration. This method was employed to reduce the extent of smear zone as much as possible.

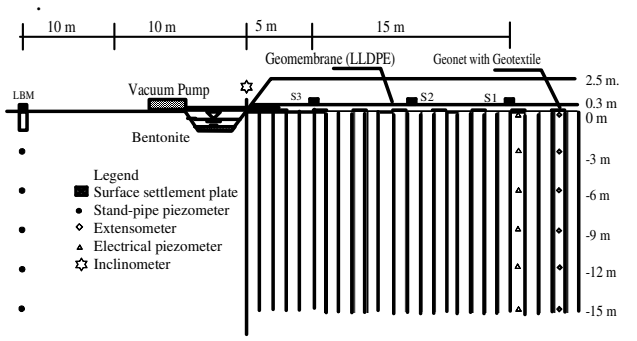

Figure 11: Cross section of embankment TV1 and location of monitoring system (Indraratna et al., 2005d)

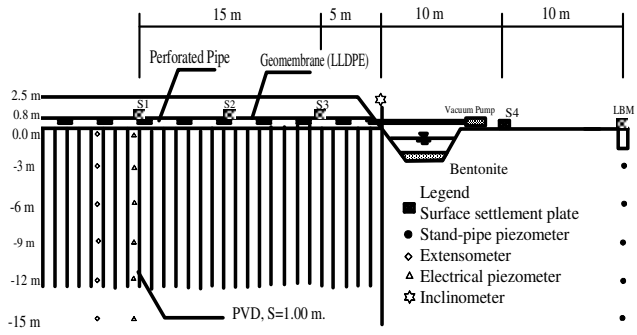

Figure 12: Cross section of embankment TV2 and location of monitoring system (Indraratna et al., 2005d)

Table 1. Vertical drain parameters

Spacing, S	1.0 m (triangular)
Ratio of k_h/k'_h	10
Diameter of drain, d_w	50 mm
Discharge capacity, q_w	50 m^3/year (per drain)
Length of vertical drain	15 m for TV1 and 12 m for TV2

The extent of the smear zone with depth was predicted using the cavity expansion theory as explained in Section 4, incorporating the Modified Cam clay parameters given in Table 2. The predicted normalized pore water pressure (i.e., u/σ_{v0}) variation with radial distance for each soil layers is shown in Figure 13.

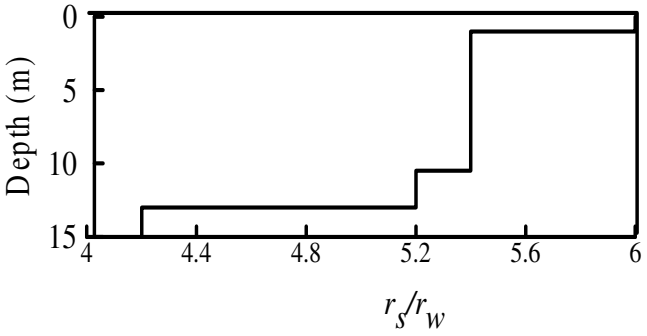

Figure 13: Variation of smear zone with depth by the Cavity Expansion theory (where, r_s: radius of smear zone, and r_w: radius of drain)

Table. 2 Soil parameters used in the analysis

Depth m	C_r	C_c	k_h $\times 10^{-9}$ m/s	e_0	γ kN/ m^3	P'_c kPa
0.0-2.0	0.06	0.37	30.1	1.8	16	58
2.0-8.5		1.6	12.7	2.8	15	45
8.5-10.5		1.7	6.02	2.4	15	70
10.5-13		0.95	2.56	1.8	16	80
13-15		0.88	0.60	1.2	18	90

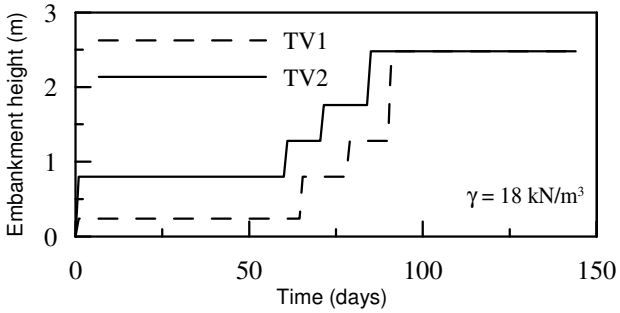

Figure 14: Multi-stage loading for embankments TV1 and TV2 (Indraratna et al., 2005d)

In each embankment, a vacuum pressure up to 70kPa could be achieved using the available vacuum equipment. This pressure is equivalent to a fill height of 4m. After 45 days of vacuum application, the surcharge load was applied in 4 stages upto 2.5m high (the unit weight of surcharge fill is 18 kN/m^3) as illustrated in Fig. 14. The settlement, excess pore water pressure, and lateral movement were observed for 5 months. During the application of vacuum pressure, it was found that the suction head transmitted to the soil could not be constantly maintained as shown in Fig. 15 (Sangmala, 1997). This fluctuation has been was attributed to air leaks through the surface membrane or the loss of suction head beneath the certain depth for long PVD. Intersection of natural macropores with drains at various depths also lead to suction head drops, at various times.

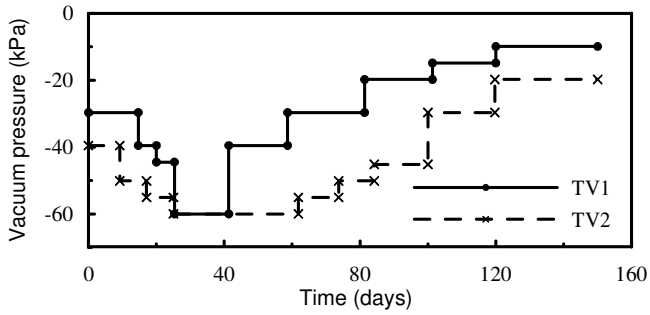

Figure 15: Time dependent vacuum pressure (Indraratna et al., 2005d)

6.3 *Single drain analysis at the embankment centreline using proposed analytical model*

In the field, at the embankment centreline (exploiting symmetry), the condition of 3-D axisymmetric consolidation without lateral strain assumed in the proposed analytical model can be justified. The soil parameters, the in-situ effective stress and the soil permeability for soft Bangkok clay subsoils are shown in Table 2. The relevant soil properties were obtained from CK_oU triaxial tests (AIT, 1995). As suggested by Tavenas et al. (1983), the slope of e-logk_h (C_k) can be determined by:

$$C_k = 0.5e_0 \tag{30}$$

In the analysis, each subsoil layer was divided into smaller sublayers to derive a more accurate effective stress distribution with depth. The value of soil compressibility index (C_k) is associated with the actual stress state within a given region of the foundation, where the working stress range must be considered in relation to the preconsolidation pressure of soil at that particular depth (Indraratna et al., 1994). The values of k_h/k_s for this case study were assumed to be 2, whereas d_s/d_w is detemined by the cavity expansion theory (Fig. 13).

The embankment loading was simulated by assuming an instantaneous loading at the upper boundary. Settlement predictions were carried out at the embankment centerline using the authors' analytical model (e.g. Eqs. 8-14). At the beginning of the subsequent stage, the initial in-situ effective stress and initial coefficient of horizontal consolidation (c_{hi}) were calculated based on the final degree of consolidation of the previous loading stage. An EXCEL spreadsheet formulation can be conveniently employed in the calculation. The value of soil compressibility (C_c or C_r) in association with the correct working effective stress plays a very important role for predicting settlement. For Stage 1 loading, where the effective preconsolidation pressure (p'_c) is not exceeded, the value of recompression index (C_r) may be used. In particular, the surface crust is heavily overconsolidated (upto about 2 m depth). Once p'_c is exceeded, the value of compression index (C_c) follows the normally consolidated line as indicated by the values in Table 2. The time-dependent vacuum pressure is assumed to vary linearly to zero along the drain length ($k_1 = 0$).

Figures 16 and 17 compare predicted surface centreline settlement with the measured data for Embankment TV1 and TV2, respectively. As expected, the predicted results based on the authors' solutions agree well with the measured results, whereas the prediction based on the constant k_h and smear zone overestimates settlement after 80 days, because, the actual soil permeability decreases significantly at higher stress levels. It is verified that the combined vacuum application and the PVD system accelerates consolidation, while the vacuum pressure acts as an additional surcharge load. As shown in Figs. 16 and 17, 'no leakage' condition gives more settlements, whereas the prediction without any vacuum application gives less settlement. It indicates that performance of this system depends entirely on preventing airleaks and the distribution of vacuum pressure along the length of the drain.

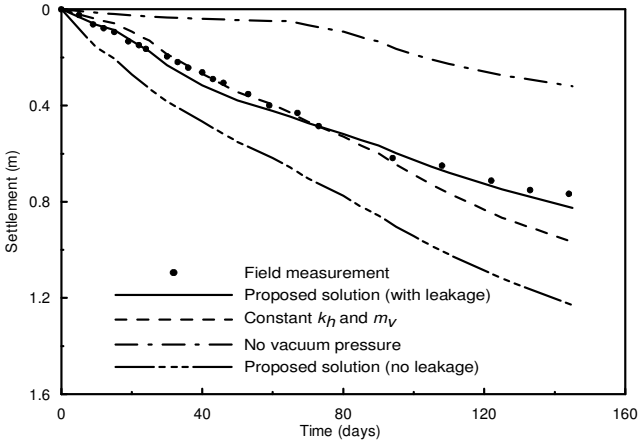

Figure 16: Surface settlement predictions at the centerline of Embankment TV1 (after Rujikiatkamjorn, 2005)

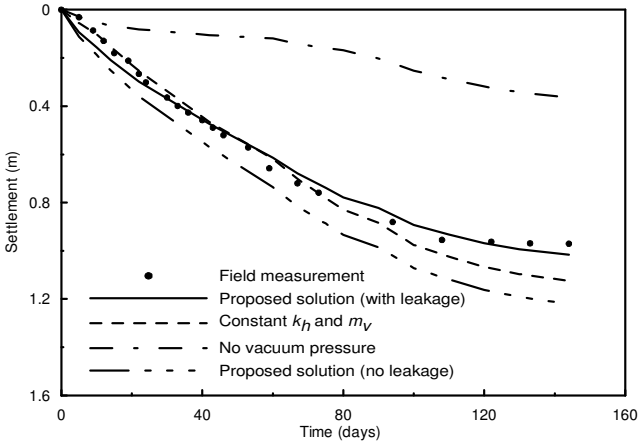

Figure 17: Surface settlement predictions at the centerline of Embankment TV2 (after Rujikiatkamjorn, 2005)

6.4 *Multi-drain analysis using FEM incorporating proposed equivalent plain strain model*

In order to investigate the performance of a whole embankment, the consolidation behaviour was analysed using the finite element software ABAQUS (Indraratna et al., 2005d). The *equivalent* plane strain model (Eqs.. 20-21) as well as the modified Cam-clay theory (Roscoe and Burland, 1968) were incorporated in the analysis. According to Indraratna and Redana (1997), the ratios of k_h/k_s and d_s/d_w determined in the laboratory are approximately 1.5-2.0 and 3-4, respectively, but in practice these ratios can vary from 1.5 to 6 depending on the type of drain, mandrel size and shape and installation procedures used (Indraratna and Redana, 2000; Saye, 2003). The constant values of k_h/k_s and d_s/d_w (Table 6.3) for this case study were assumed to be 2 and 6, respectively (Indraratna et al., 2004). For the plane strain FEM simulation, the equivalent permeability inside and outside the smear zone was determined using Eqs. (20) and (21). The discharge capacity (q_w) is assumed high enough and can be neglected (Indraratna and Redana, 2000).

The finite element mesh contained 8-node bi-quadratic displacement and bilinear pore pressure elements (Fig. 18). Only the right hand side of the embankment was modeled due to symmetry, as shown in Fig. 18. For the PVD zone and smear zone, a finer mesh was implemented so that each unit cell represented a single drain with the smear zone established on either side. The finer mesh was imperative to prevent an unfavorable aspect ratio of the elements (Indraratna and Redana, 2000). The different drain lengths for the two embankments were modelled by fixing the pore pressure boundary along the appropriate depths. The incremental surcharge loading was simulated at the upper boundary.

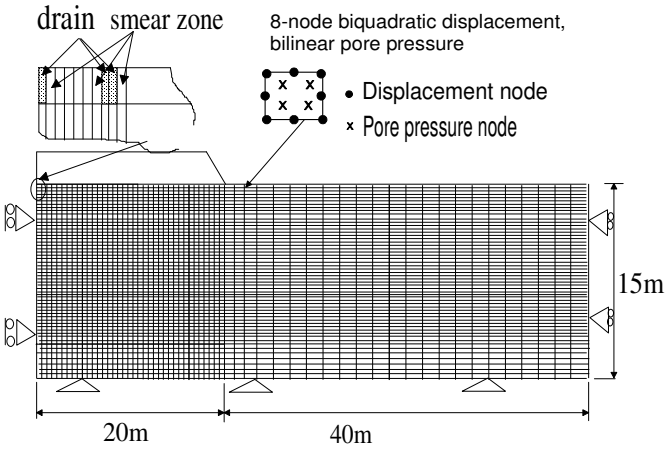

Figure 18: Finite element mesh for plane strain analysis (modified after Indraratna et al. 2005f)

The following 4 distinct models were numerically examined under the 2D multi-drain analysis (Indraratna et al. 2005f):

Model A: Conventional analysis (i.e., no vacuum application),

Model B: Vacuum pressure varies according to field measurement and decreases linearly to zero at the bottom of the drain (k_1= 0),

Model C: No vacuum loss (i.e. -60kPa vacuum pressure was kept constant after 40 days); vacuum pressure diminishes to zero along the drain length (k_1= 0),

Model D: Constant time-dependent vacuum pressure throughout the soil layer (k_1=1).

All the above models included the smear effect but neglected well resistance as previous studies indicated that well resistance was not significant for drain lengths shorter than about 20m (Indraratna & Redana, 2000). For embankment TV2 with 12m drain length, pore pressure at the drain interface was fixed up to 12m depths only.

Figures 19 and 20 compare surface settlement between prediction and measurement (centreline) for embankment TV1 and TV2, respectively. Model B predictions agree with the field data. Comparing all the different vacuum pressure conditions, Models A and D give the lowest and highest settlement, respectively. A vacuum application combined with a PVD system can accelerate the consolidation process significantly. With vacuum application, most of the primary consolidation is achieved around 120 days, whereas conventional surchage (same equivalent pressure) requires more time to complete primary consolidation (after 150 days). It is also apparent that a greater settlement can be obtained, if any loss of vacuum pressure can be minimised (Model C).

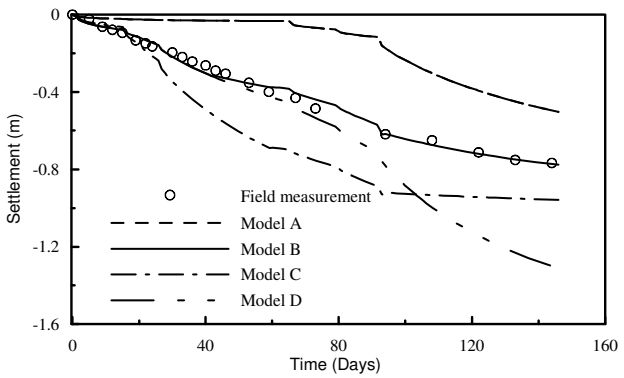

Figure 19: Surface settlement time curves of embankment TV1 (modified after Indraratna et al., 2005f)

Figures 21 and 22 illustrate the predicted and measured excess pore pressures for embankments TV1 and TV2 respectively. The field observations are closest to Model B, implying that the writers assumption of linearly decreasing time-dependent vacuum pressure along the drain length is justified. Excess pore pressure generated from the vacuum application is less than the conventional case, which enables the rate of construction of an embankment to be higher than conventional construction.

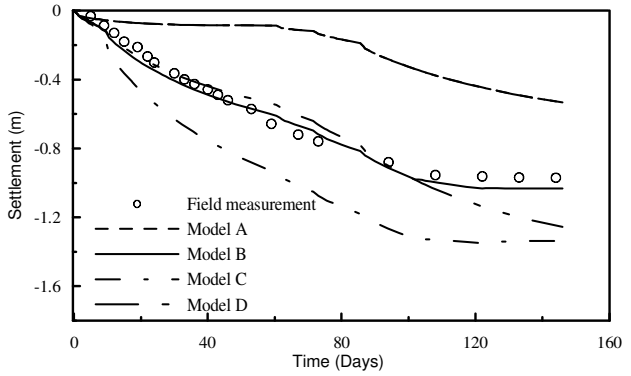

Figure 20: Surface settlement of embankment TV2 (modified after Indraratna et al., 2005f)

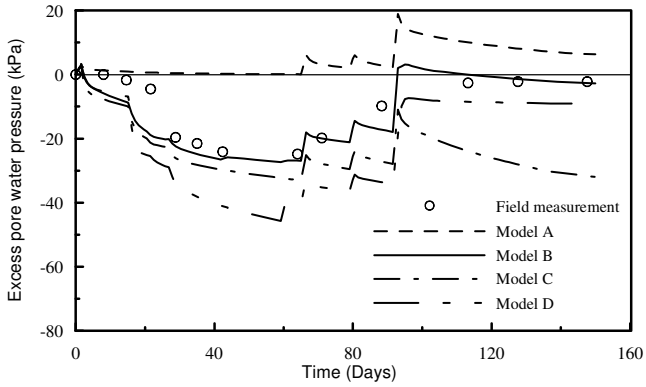

Figure 21: Variation of excess pore water pressure 3m deep below the surface and 0.5m away from centreline for Embankment TV1 (modified after Indraratna et al., 2005f)

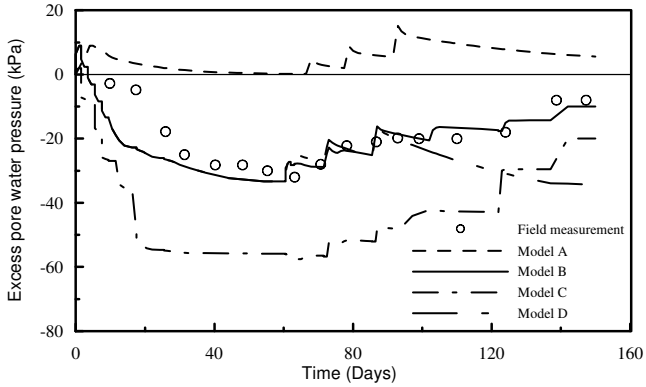

Figure 22: Variation of excess pore water pressure at 3m below the surface and 0.5m away from centreline for Embankment TV2 (modified after Indraratna et al., 2005f)

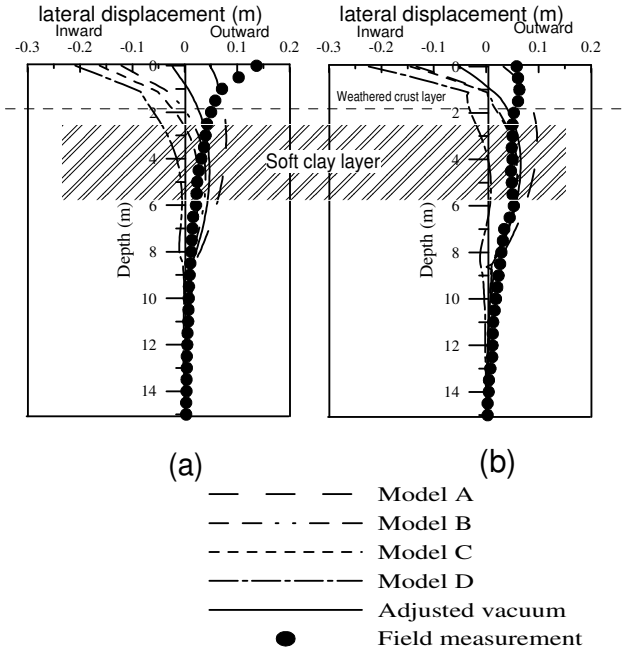

Figure 23: Calculated and measured lateral displacements distribution with depth (a) embankment TV1 (b) embankment TV2 (modified after Indraratna et al., 2005f)

The predicted and measured lateral displacements (at the end of embankment construction) are shown in Fig. 23. The observed lateral displacements do not agree well with all vacuum pressure models. In the middle of the very soft clay layer (4-5m deep), the predictions from Models B and C are closest to the field measurements. Nearer to the surface, the field observations do not agree with the 'inward' lateral movements predicted by Models B and C. The discrepancy between the finite element models and the measured results is more evident in the topmost weathered crust (0-2 m).

7 SUMMARY AND CONCLUSIONS

The use of prefabricated vertical drains, their properties and associated merits and demerits have been discussed. In this paper, the extent of smear zone can be predicted by the cavity expansion theory and validated by large scale laboratory results based on the variation of water content and soil permeability. It is found that soil unsaturation at the vertical drain boundary due to mandrel driving could delay the excess pore pressure dissipation in the early stage of consolidation process. The behaviour of soft clay under the influence of PVD and vacuum application was described on the basis of numerous case histories where both field measurements and predictions were available.

An analytical model incorporating vacuum preloading has been described for both axisymmetric and equivalent plane strain conditions. A finite element code (ABAQUS) was employed to analyse the unit cell and compare the

numerical results with the analytical approach. A conversion procedure based on the transformation of permeability and vacuum pressure was introduced to establish the relationship between the axisymmetric (3D) and equivalent plane strain (2D) conditions. The plane strain solution was applied for case history analysis, proving its validity to predict real behaviour. Field behaviour as well as model predictions indicate that the efficiency of vertical drains depends on the magnitude and distribution of vacuum pressure.

An accurate prediction of lateral displacement depends on the careful assessment of soil properties including the overconsolidated surface crust. This compacted layer is relatively stiff, and therefore it resists 'inward' movement of the soil after vacuum application. Clearly, the modified Cam-clay model is inappropriate for modeling the behavior of a weathered and compacted crust. It may be better modeled as an elastic layer rather than a 'soft' elasto-plastic medium. An analysis of the case histories showed that the vacuum application via PVD substantially decreases lateral displacement, thereby reducing potential shear failure during rapid embankment construction.

There is no doubt that a system of vacuum-assisted consolidation via PVD is a useful and practical approach for accelerating radial consolidation. Such a system reduces the need for a high surcharge load, as long as air leaks can be eliminated in the field. Accurate modeling of vacuum preloading requires laboratory and field studies to investigate the exact nature of vacuum pressure distribution within a given soil formation and PVD system. In addition, a resilient system is required to prevent air leaks that can reduce the desirable negative pressure (suction), with time.

8 ACKNOWLEDGEMENT

The authors wish to thank the CRC for Railway Engineering and Technologies (Australia) for its continuous support and the Thailand Airport Authority for providing the trial embankments data. The Cavity Expansion Theory application to PVDs was the result of a PhS study by Dr. I. Sathananathan. In addition, assistance of Prof. A.S. Balasubramaniam (formerly at Asian Institute of Technology, Bangkok, Thailand) is gratefully appreciated. A number of past research students of Prof. Indraratna, namely, Sathananathan, Redana, Bamunawita, Balachandran, and Ratnayake, have also contributed to the contents of this keynote paper through their research work.

Much of the contents reported in this paper are described in greater details in a number of Canadian Geotechnical and ASCE Journal of primary author as listed in the references.

REFERENCES

AIT. 1995. The Full Scale Field Test of Prefabricated Vertical Drains for The Second Bangkok International Airport (SBIA). AIT,Bangkok, Thailand.

Barron, R.A., 1948. Consolidation of fine-grained soils by drain wells. *Transactions ASCE*, Vol 113, paper 2346: 718-724.

Chai, J. C., Miura, N., Sakajo, S., and Bergado, D. T. 1995. Behavior of vertical drain improved subsoil under embankment loading. *J. Soil and Foundations, Japanese Geotechnical Society*, 35(4), 49-61.

Chu, J., Yan, S. W., and Yang, H. 2000. Soil improvement by the vacuum preloading method for an oil storage station. *Geotechnique*, 50(6), 625-632.

Cognon, J. M., Juran, I and Thevanayagam, S., 1994. Vacuum consolidation technology- principles and field experience, *Proceedings of conference on vertical and horizontal deformations of foundations and embankments deformations*, College station, Texas.

Hansbo, S. 1981. Consolidation of fine-grained soils by prefabricated drains. *In Proceedings of 10th International Conference on Soil Mechanics and Foundation Engineering, Stockholm, Balkema, Rotterdam*, 3, pp. 677-682.

Hird, C.C., Pyrah, I.C., and Russell, D. 1992. Finite element modelling of vertical drains beneath embankments on soft ground. *Geotechnique*, 42(3): 499-511.

Indraratna, B., Balasubramaniam, A. S., and Balachandran, S. 1992. Performance of test embankment constructed to failure on soft marine clay. *J. Geotech. Eng., ASCE*, 118, 12-33.

Indraratna, B., Balasubramaniam, A. S., and Ratnayake, P. 1994. Performance of embankment stabilized with vertical drains on soft clay. *J. Geotech. Eng., ASCE*, 120(2), 257-273.

Indraratna, B., Balasubramaniam, A. S., and Sivaneswaran, N. 1997. Analysis of settlement and lateral deformation of soft clay foundation beneath two full-scale embankments. *Int. J. for Numerical and Analytical Methods in Geomechanics*, 21, 599-618.

Indraratna, B., Bamunawita, C., and Khabbaz, H. 2004. Numerical modeling of vacuum preloading and field applications. *Canadian Geotechechnical Journal*, 41, 1098-1110.

Indraratna, B., and Redana, I. W. 1995. large-scale, radial drainage consolidometer with central drain facility. *Australian Geomechanics*, 29(103-105).

Indraratna, B., and Redana, I. W. 1997. Plane strain modeling of smear effects associated with vertical drains. *J. Geotech. Eng., ASCE*, 123(5), 474-478.

Indraratna, B., and Redana, I. W. 1998. Laboratory determination of smear zone due to vertical drain installation. *J. Geotech. Eng., ASCE*, 125(1), 96-99.

Indraratna, B., and Redana, I. W. 2000. Numerical modeling of vertical drains with smear and well resistance installed in soft clay. *Canadian Geotechnical Journal*, 37, 132-145.

Indraratna, B., Rujikiatkamjorn C., and Sathananthan, I. 2005a. Analytical and numerical solutions for a single vertical drain including the effects of vacuum preloading. *Canadian Geotechinical Journal*, 42: 994-1014.

Indraratna, B., Rujikiatkamjorn C., and Sathananthan, I. 2005b. Radial consolidation of clay using compressibility indices and varying horizontal permeability. *Canadian Geotechinical Journal*, 42: 1330-1341.

Indraratna, B., Rujikiatkamjorn C., and Sathananthan, I., 2005c. Analytical modeling and field assessment of embankment stabilized with vertical drains and vacuum preloading. *The Proceedings of the 16th International Conference on Soil Mechanics and Geotechnical Engineering*, 12-16 September 2005, Osaka, Japan, Edited by the 16th ICSMGE committee, Millpress, Rotterdam, the Natherlands, 1049-1052.

Indraratna, B., Rujikiatkamjorn C., Balasubramaniam, A. S. and Wijeyakulasuriya, V. 2005d. Predictions and observations of soft clay foundations stabilized with geosynthetic drains and vacuum surcharge. *Ground Improvement – Case Histories Book* (Volume 3), Edited by Indraratna, B. and Chu, J., Elsevier, London, 199-230.

Indraratna, B., Sathananthan, I., Bamunawita, C. and A.S. Balasubramaniam. 2005e. Theoretical and Numerical Perspectives and Field Observations for the Design and Performance Evaluation of

Embankments Constructed on Soft Marine Clay. *Ground Improvement–Case Histories Book* (Volume 3), Edited by Indraratna, B. and Chu, J., Elsevier, London, Chapter 2:61-106.

Indraratna, B., Sathananthan, I., Rujikiatkamjorn C. and Balasubramaniam, A. S. 2005f. Analytical and numerical modelling of soft soil stabilized by PVD incorporating vacuum preloading. *International Journal of Geomechanics*, Vol. 5 No. 2, 114-124.

Indraratna, B., Rujikiatkamjorn C., Sathananthan, I., Shahin, M.A., and Khabbaz, H. 2005g. Analytical and numerical solutions for soft clay consolidation using geosynthetic vertical drains with special reference to embankments. *The Fifth International Geotechnical Engineering Conference*, Cairo, 55-86.

Jamiolkowski, M., Lancellotta, R., and Wolski, W. 1983. Precompression and speeding up consolidation. In Proceedings of 8th European Conference on Soil Mechanics and Foundoundtions, Helsinki, Finland, 3, 1201-1206.

Johnson, S.J. 1970. Precompression for improving foundation soils. *J. Soil. Mech. Found. Div., ASCE*, 96(1):111-114.

Kjellman, W. 1952. Consolidation of clayey soils by atmospheric pressure. *Proceedings of a conference on soil stabilization*, Massachusetts Institute of Technology, Boston, 258-263.

Lekha, K. R., Krishnaswamy, N. R., and Basak, P. (2003). Consolidation of clays for variable permeability and compressibility. *Journal of Geotechnical and Geoenvironmental Engineering, ASCE*, 129(11), 1001-1009.

Nagaraj, T. S., Pandiam, N. S., and Narasimha Raju, P. S. R. 1994. Stress-state-permeability relations for overconsolidated clays. *Geotechnique*, 44(2), 349-352.

Qian, J. H., Zhao, W. B., Cheung, Y. K., and Lee, P. K. K. 1992. The theory and practice of vacuum preloading. *Computers and Geotechnics*, 13, 103-118.

Roscoe, K.H., and Burland, J.B. 1968. On the generalized stress strain behavior of wet clay. *Engineering plasticity*, Cambridge Univ. Press; Cambridge, U.K., 535-609.

Rujikiatkamjorn. 2005. Analytical and numerical modelling of soft clay foundation improvement via prefabricated vertical drains and vacuum preloading. *PhD Thesis*, Universtiy of Wollongong, 263p.

Sangmala, S., 1997. Efficiency of drainage systems of vacuum preloading with surcharge on PVD improved soft Bangkok clay, *ME Thesis*, Asian Institute of Technology, Bangkok, Thailand.

Saye, S. R. 2003. Assessment of soil disturbance by the installation of displacement sand drains and prefabricated vertical drains. *Geotechnical Special Publication No. 119, ASCE*, 325-362.

Sathananthan, I. 2005 Modelling of Vertical Drains with Smear Installed in Soft Clay. *PhD Thesi*s, Universtiy of Wollongong, 264p.

Sathananthan, I. and Indraratna, B. 2006. Laboratory Evaluation of Smear Zone and Correlation between Permeability and Moisture Content. Submitted to Journal of Geotechnical and Geoenvironmental Engineering, ASCE (in press).

Seah, T. H., and Juirnarongit, T. 2003. Constant rate of strain consolidation with radial drainage. *Geotechnical Testing Journal*, 26(4), 1-12.

Tang, M., and Shang, J. Q. 2000. Vacuum preloading consolidation of Yaoqiang Airport runway. *Geotechnique*, 50(6), 613-623.

Tavenas, F., Jean, P., and Leroueil, S. 1983. The permeability of natural soft clays, Part 2: Permeability characteristics. *Canadian Geotechechnical Journal*, 20, 645-660.

Yan, S. W., and Chu, J. 2003. Soil improvement for a road using a vacuum preloading method. *Ground Improvement*, 7(4), 165-172.

Yoshikuni, H., and Nakanodo, H. 1974. Consolidation of Fine-Grained Soils by Drain Wells with Finite Permeability. *Japan Soc. Soil Mech. and Found. Eng*, 14(2), 35-46.